

Large-scale quasi-steady modelling of a downburst outflow using a slot jet

W. E. Lin[†] and E. Savory[‡]

*Department of Mechanical & Materials Engineering,
The University of Western Ontario, London, Ont., Canada, N6A 5B9
(Received June 22, 2006, Accepted September 22, 2006)*

Abstract. This article synthesizes the literature on the meteorology, experimental simulation, and wind engineering ramifications of intense downburst outflows. A novel design of a large-scale test facility and experimental evidence of its validity are presented. A two-dimensional slot jet is used to simulate only the outflow region of a downburst. Profiles of mean velocity and turbulence quantities are acquired using hot-wire anemometry. Comparison with the literature provides empirical evidence that supports the current approach. A geometric analysis considers the validity of applying a two-dimensional approximation for downburst wind loading of structures. This analysis is applicable to power transmission lines in particular. The slot jet concept can be implemented in a large boundary layer wind tunnel to enable large-scale laboratory experiments of thunderstorm wind loads on structures.

Keywords: downburst outflow; microburst outflow; localized intense wind; thunderstorm wind load; large-scale wind tunnel; two-dimensional wall jet; slot jet; frontal curvature.

1. Introduction

Downbursts are sudden, intense downdrafts in thunderstorms that are known to persist to ground level. After impinging on the ground, a horizontal flow spreads outwards from the downdraft column. The downdraft and outflow are often assumed to be axisymmetric and the dominant outflow velocity component is in the radial direction.

The history of downburst research is well documented by the meteorological community (Wilson and Wakimoto 2001, Hjelmfelt 2003). Early studies were concerned with the downburst as an aviation hazard. Fujita (1990) summarizes his findings and addresses wind engineers, who are primarily concerned with damage to the built environment by the outflow region (Selvam and Holmes 1992, Nicholls, *et al.* 1993, Letchford, *et al.* 2002). Fujita and Wakimoto (1981) describe downburst clusters on 16 July 1980 that caused \$650 million of damage in Wisconsin, Illinois and Michigan.

Exposure of power transmission systems to damaging winds is of particular concern, since line targets are at greater risk of exposure than point targets. Risk models find that the return period for

[†] Graduate Student, Corresponding Author, Email: wlin25@uwo.ca

[‡] Associate Professor, Email: esavory@eng.uwo.ca

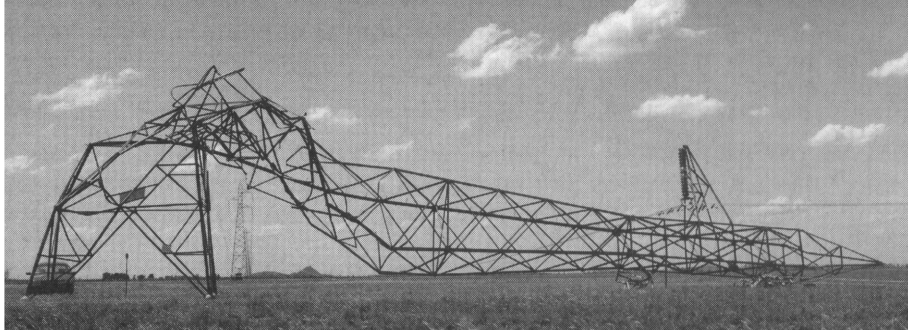


Fig. 1 Tower failure north of Bendigo, Australia in 1993 (Holmes 2001)

intersection of a transmission line by a storm is inversely proportional to the length of the line (Holmes 1999). Qualitative assessments of tower damage and aerial surveys of debris scatter patterns suggest downbursts have caused catastrophic failure of transmission line towers throughout the world, as depicted in Fig. 1.

Fieldwork utilizing Doppler radar networks proved the existence of the downburst, and documented its structure and morphology. Key studies include Northern Illinois Meteorological Research On Downburst (NIMROD) and the Joint Airport Weather Studies (JAWS) project in Colorado (Wakimoto 1982, Wilson, *et al.* 1984, Fujita 1985, Hjelmfelt 1988). In the NIMROD study, three Doppler radars were located far apart from each other (≈ 60 km) in order to increase the likelihood of detection. This preliminary study provided direct evidence of the existence of downbursts by detecting close to 50 events during the spring and summer of 1978. With spacings of 15–28 km between radars, the subsequent JAWS study produced well-defined vector plots of the horizontal mean velocity field¹, showed the variability of the reconstructed 3-D wind field from event to event, and corroborated that downburst occurrence was more common than previously thought.

However, the majority of recorded downbursts in these studies are not of damaging intensity. The peak wind speeds recorded in NIMROD and JAWS downbursts, as indicated by the horizontal lines in Fig. 2, are mostly less than F1 on the damage specification F-scale (Fujita 1981). Likely structural damage is expected at F1 and greater. The largest speeds reported for 50 NIMROD and 186 JAWS downbursts were only 31.3 and 32.6 m/s, respectively. More observational data from the extreme events would help to verify Fujita's projection of exponential decrease in annual frequency as intensity increases. Nonetheless, the estimate that four events as intense as the Andrews Air Force Base (AFB) downburst occur annually in the contiguous United States does not seem unreasonable. A propeller anemometer recorded a remarkable peak wind speed of 67 m/s at 4.9 m above ground level (AGL) during this event (Fujita 1985). As well, the projected annual frequency of events capable of structural damage is not trivial.

For clarity, "peak" wind speed will refer to the peak value in time at a fixed spatial location (e.g. in a propeller anemometer record as shown as Fig. 3). There is no time dependency in a quasi-

¹Although vector plots of radar data often are reported with a specific time noted, it is likely that these fields are not precisely instantaneous and scanning time has been accounted for somehow in post-processing of the data. Also, they do not reveal much turbulence information, which is of interest for wind tunnel simulations.

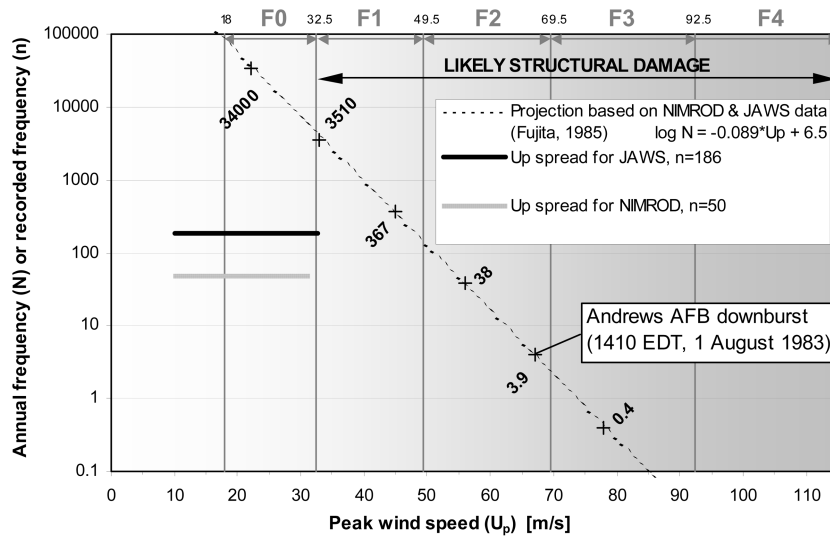


Fig. 2 Expected annual and recorded frequencies for downbursts of various intensities

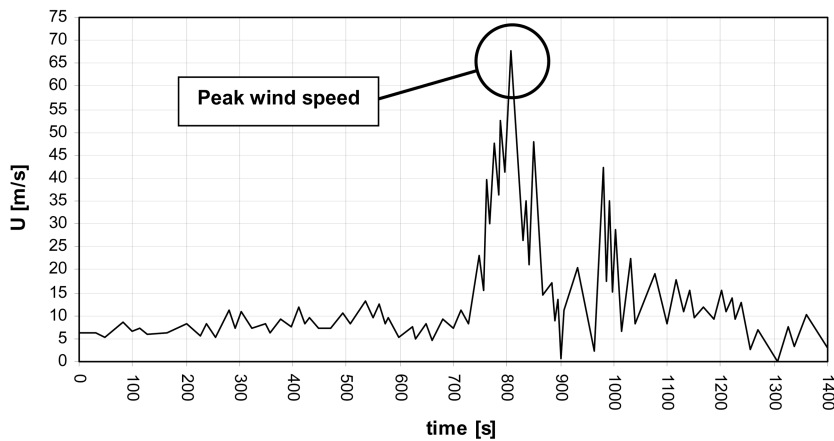


Fig. 3 Time history at a point in the Andrews AFB downburst (data reproduced from Fujita 1985)

steady model and the present work primarily deals with the maximum value in space, which will be referred to as “maximum” wind speed. The peak maximum velocity of an outflow is of primary interest for structural loading.

In practice, the full-scale 3-D wind field is approximately reconstructed and a stationary downburst is modelled as an axisymmetric flow. Probes along the height of a tower can give the vertical variation of velocity in the outflow. Full-scale estimate of the radial variation of velocity is more difficult. Since previous work will have used different measurement methods, “reported maximum” will refer to the largest value reported in a given study.

Several factors make observation of extreme events, such as the Andrews AFB downburst, difficult. Compared to typical meteorological scales, the duration and spatial extent of a strong downburst outflow are brief and small, respectively. Near-peak winds lasting more than 5 minutes

are considered long-lived and strong outflows generally affect a region of 0.4–4 km diameter². As well, active storm regions such as the Canadian Prairie provinces and the American Midwestern states have relatively low population density, which likely results in unobserved downbursts or their mistaken identification as tornadoes (Fujita 1981).

Dedicated radar stations at sufficiently close spacing can resolve the low-level kinematic structure of downbursts. However, technological challenges for detection include contamination of radar echoes by ground clutter and a lack of tracer particles in dry downbursts. Some of the strongest downbursts analyzed by Hjelmfelt (1988) occurred with very low reflectivity at the velocity maximum. This characteristic would make it difficult to forecast and study damaging outflows.

Despite these limitations on fieldwork, the motivation to understand extreme weather phenomena is provided by their significant damage potential. Full-scale observation can be supplemented with laboratory simulation when the controlled flow shows acceptable agreement with available full-scale data. Building on the early interest regarding the downdraft and touchdown region, recent work has focussed on the outflow near ground level.

However, with existing methods, a tremendous amount of laboratory space would be required to simulate the entire outflow region on a physical scale that is amenable to wind loading and aeroelastic testing of models. The round impinging jet approach yields a height to the maximum outflow velocity, at the radial location where maximum outflow velocity occurs, of less than 3% of the initial jet diameter. The largest impinging jet facility found in the literature creates a 1.60 m diameter downdraft (Sarkar and Haan, Jr. 2002). As well, simulating additional full-scale features such as downburst translation has proven problematic. Translation of a large nozzle is described as unwieldy or “clumsy” (Mason, *et al.* 2003).

The impinging jet approach is a logical way to achieve flow similarity. However, the present work seeks a better solution to the practical engineering problem of generating a large-scale flow that is very similar to a downburst outflow. Also, the proposed approach is readily refined to allow additional features to be added to the simulated outflow velocity profile, such as a translating or wind shear component.

2. Key considerations for outflow simulations

The following issues need to be addressed in simulations of the downburst outflow:

a) As recognized by Selvam and Holmes (1992), the vertical profile of radial wind speed has a different shape than that of the conventional atmospheric boundary layer (ABL). Fig. 4 depicts the characteristic vertical profile of mean velocity associated with the downburst outflow. Maximum velocity occurs near ground level and decreases with further increase in height. The ABL profile increases monotonically with height and is commonly modelled with either a power or logarithmic law equation (ASCE 1999). For lattice tower designs in which specific members are designed for a specific load case, this difference in the vertical variation of the wind load may be critical.

b) A quasi-steady model neglects the evolution in time of the outflow and simply assumes a steady velocity profile. The early experiments, related to wind engineering applications, were developed on this basis (Holmes 1992, Letchford and Illidge 1999, Wood, *et al.* 2001). The quasi-steady approach is the focus of this article.

²Microbursts have this spatial extent. The more general term “downburst” is used in this article for simplicity.

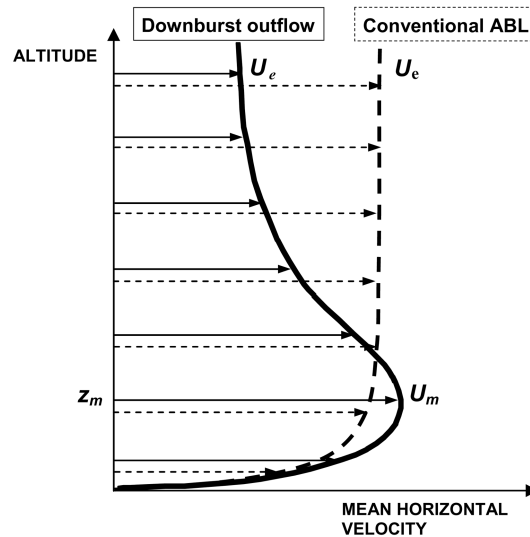


Fig. 4 Comparison of profile shapes for a typical atmospheric boundary layer wind and a downburst outflow

c) More accurate models consider the transient nature of the outflow. From the perspective of a stationary object, a downburst outflow passes by as a sudden and short-lived event. Anemometer records of the outflow show a sharp rise in velocity with near-peak winds generally lasting less than 5 minutes, as indicated by full-scale time histories (Fujita 1985, Gast and Schroeder 2003). Recent advances in wind tunnel simulation beyond a simple quasi-steady approach are discussed in a forthcoming companion article by the authors, where the present slot jet approach is developed further to incorporate transient wind effects. Reference to transient simulations is kept to a minimum in this article to avoid needless repetition.

d) A primary vortex ring that expands radially outward from the central axis of the downdraft is a dominant feature in the outflow region (Fujita 1985, Hjelmfelt 1988). Near the ground plane, the circulating fluid of the vortex ring moves in the same outward direction as the divergent impinging flow, so maximum outflow velocities are expected there (Proctor 1988). This vortex ring may cause a significant vertical velocity component in the outflow. Comparison of the instantaneous vertical profile of radial velocity of a transient impinging jet (Mason, *et al.* 2005) to the time-averaged vertical profile of radial velocity of a steady impinging jet (Chay and Letchford 2002) show significant differences in profile shape and suggest that the vortex ring leads to higher peak maximum velocities.

e) Since the downburst outflow event is a non-stationary process, it is problematic to quantify the downburst outflow gustiness using the traditional definition of turbulence intensity. As proposed by Choi and Hidayat (2002), assessment of the variations about a moving average seems to be more appropriate. Their approach allows an effective turbulence intensity to be determined.

f) Local surface flows with reported speeds of up to 11 m/s (Hjelmfelt 1988) may distort the idealized, axisymmetric flow and cause a pronounced directionality of the outflow, which is associated with tilting of the downdraft from the vertical. As well, the overall motion of the parent storm is thought to translate embedded downbursts. Assuming superposition of the storm translation velocity onto the axisymmetric model flow field, the maximum velocities are expected to be in the direction of the storm motion and just behind the leading edge of the translating downburst (Fujita

1981). A simulation facility should have the capability to model both stationary and translating events.

The present work focusses on the first two items above. By extension of the present approach, the other considerations are discussed in a forthcoming companion article. An actuated control gate is added to the test facility described in Section 3.3.

3. Experimental methodology

As noted by Hjelmfelt (1988), the downburst profile bears a strong resemblance to the classical wall jet. Wall jet simulations in a controlled environment are reproducible and allow more detailed measurements than in field studies. They provide useful results and are an indirect means of addressing the fieldwork limitations discussed in Section 1.

3.1. Previous approaches

Previous downburst experiments use one of the two following methods. Investigations of downburst morphology and structure have been conducted at very small geometric and velocity scales by the release of a liquid mass into a larger body of less dense liquid (Lundgren, *et al.* 1992, Alahyari and Longmire 1995, Yao and Lundgren 1996). This approach is not suitable for wind loading studies on models. Larger scale simulations use an impinging jet as shown in Fig. 5 (Letchford and Illidge 1999, Wood, *et al.* 2001, Chay and Letchford 2002, Xu 2004).

A centrifugal fan is typically used to drive air through a circular nozzle. Flow conditioning devices are located between the fan and nozzle. The flow travels from the nozzle towards the impingement plane as an axisymmetric free jet. Measurements by Chay and Letchford (2002) indicate that the impingement region extends from the free jet axis to somewhere between $r/D_n = 1.0$ and 1.25. Xu (2004) suggests a value near $r/D_n = 1.0$, after which the wall jet develops in the radial (r) direction. The normal-to-impingement-plane profiles of mean radial velocity and turbulent quantities reach a developed state after 3.0 and 4.5 nozzle diameters downstream of the nozzle axis, respectively (Knowles and Myszko 1998). Impinging jet experiments define a jet Reynolds number (Re_d) based on nozzle diameter (D_n) and exit velocity.

Table 1 compares the key parameters from various impinging jet studies to those found in the full-scale outflow. Note that full-scale downdraft diameter (D) is a best estimate, whereas D_n is accurately known in laboratory experiments. The reported maximum radial velocities compiled in Table 1 should be treated with caution. The full-scale values are the largest reported wind speeds over time and space. However, the impinging jet studies use a continuous jet with a quasi-steady assumption, so they report a spatial maximum that has been time-averaged.

U_m occurs at z_m above the impingement plane, at the nose of the outflow/wall jet velocity profiles shown in Figs. 4 and 5. Since z_m from an impinging jet is dependent on D_n , generating a large-scale wall jet requires a tremendous nozzle diameter. The separation distance between nozzle and ground plane also increases as D_n increases, if z/D_n is to be kept similar to observed cloud base height to downdraft diameter ratios. D_n in previous studies is fairly large in terms of what is feasible in a laboratory, yet the largest z_m (at the radial position³ of reported max U as compiled in Table 1) is

³The maximum radial wind speed occurs at a specific radial distance away from the downdraft axis. Holmes and Oliver (2000) present a model for the radial decay of radial wind speed.

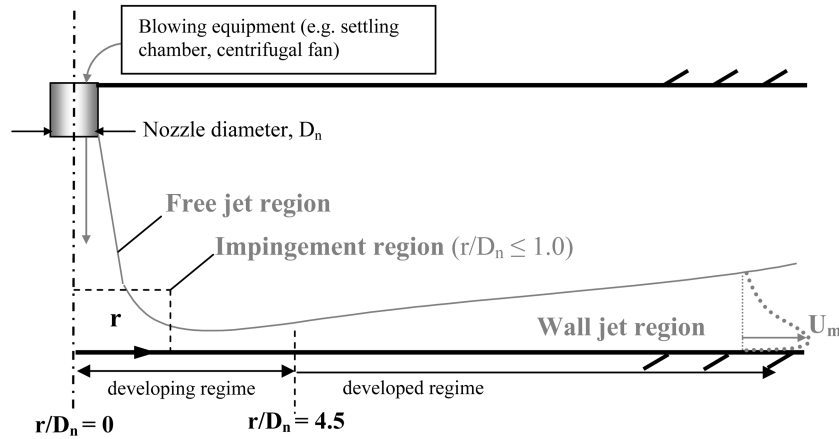


Fig. 5 Typical impinging jet experiment apparatus and nomenclature

Table 1 Comparison of parameters from full-scale and impinging jet studies

Study	Downdraft		Outflow		Comments
	diameter [m]	reported max U [m/s]	z_m [m]	radial position of reported max U	
Full-scale	D			r/D	
Fujita (1981, 1985, 1990)	2000 at $z/D \sim 0.45$	32 27	50 30	1.1 no data	Yorkville downburst. ^a (NIMROD) 29 May 1978.
Fujita (1985)	likely < 2000	likely > 67	likely > 4.9	no data	Andrews AFB downburst. 1 August 1983. Single point measurement.
Hjelmfelt (1988)	1500 – 3000 at $z = 1500$ m AGL	18	no data	0.75 – 1.0	Downdraft data from 11 events. Outflow data from 14 July D. (JAWS) June - August 1982.
Impinging jet	D_n			r/D_n	
Letchford and Illidge (1999)	1.01 at $z/D_n = 0.90$	10	≈ 0.01	1.5	Flow from wind tunnel exit with octagonal cross-section.
Wood, <i>et al.</i> (2001)	0.31 at $z/D_n = 2$	19	0.004	1	Flow from circular nozzle attached to rectangular settling chamber.
Chay and Letchford (2002)	0.51 at $z/D_n = 1.7$	10	≈ 0.006	≈ 1	Flow from circular nozzle (with lip) attached to settling chamber.
Xu (2004)	0.22 at $z/D_n = 1, 2, 3, 4$	≤ 13	< 0.006 in all cases	1	Flow from ≈ 15 m long circular pipe attached to settling chamber.

^aTwo records of the event made 6 minutes apart (Fujita 1985)

only a few centimetres.

In addition to practical space requirements, it is also difficult to refine a large-scale impinging jet to include further complexities beyond the basic stationary downburst configuration. The present approach addresses this practical engineering problem of maximizing the flow size, whilst retaining the key features of an intense downburst outflow. It is also readily extended to model the outflow from a translating event.

3.2. Present slot jet approach

By treating the outflow separately from the downdraft column, the outflow region can be simulated at a larger scale than in previous experiments. An analogous approach is well established in wind loading studies with the ABL. Wind tunnel boundary layer spectra show good agreement with full-scale data when only the lower third of the total ABL thickness is simulated at 1:100–1:250 scale (Cook 1973). Thus, a suitably large boundary layer for model testing is achieved in a wind tunnel of economical size (typically ≈ 2 m height and ≈ 10 m fetch).

The present work models the downburst outflow by introducing a strong secondary flow at the beginning of the working section of a conventional boundary layer wind tunnel. A schematic of the slot jet flow with conventional nomenclature is shown as Fig. 6. A centrifugal fan beneath the tunnel ground plane drives the flow through a rectangular slot located near the tunnel inlet. With distance downstream of the slot exit (x), velocity decays and wall jet height (δ) increases.

The development x -distance is typically normalized by the slot height, b . A slot Reynolds number (Re_j) is defined based on b and the mean velocity at the slot exit spanwise centreline ($x=0$, $y=0$). The x -distance required for the U profile to become “developed” appears to be inversely related to Re_j . Values as low as $x/b=20$ (Förthmann 1934, $Re_j=54000$) and as high as $x/b=104$ (Verhoff 1970, $Re_j=10300$) are reported. As side wall boundary layer growth becomes significant, the wall jet will lose its nominal two-dimensionality. For the present application, it is desirable to maximize Re_j and work in the 2-D region.

The wind tunnel flow may also be run simultaneously as a co-flow with the slot jet. Superposition of the co-flow and wall jet yields downstream velocity profiles that may be used to model the outflow from a translating downburst. Hjelmfelt (1988) noted local surface crossflows of up to 11 m/s in various Colorado downbursts that can contribute to the downburst outflow velocity.

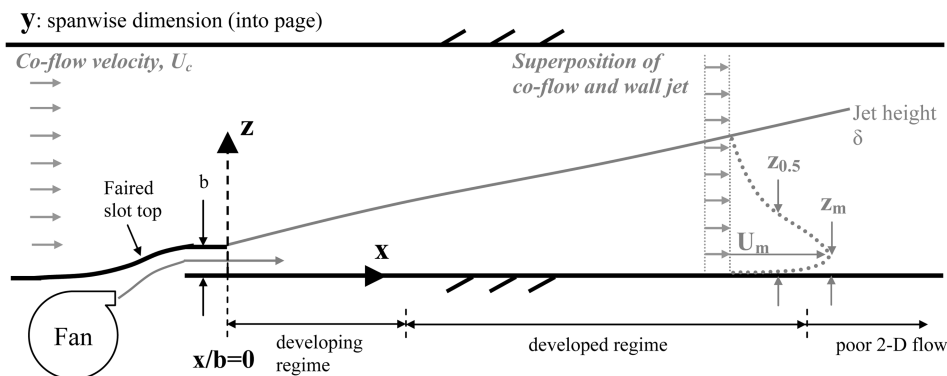


Fig. 6 Two-dimensional slot jet apparatus and nomenclature

Preliminary results in Section 4 are only with a no co-flow slot jet, which corresponds to a stationary outflow simulation. A further complexity is that the full-scale downdraft may be situated directly above a structure. Or more generally, the wind loading may have a significant vertical component. Researchers at the UWO Boundary Layer Wind Tunnel Laboratory (BLWTL) are presently designing a section model mount with three rotational degrees of freedom (Mara and Galsworthy 2006). Implemented with the slot jet approach, vertical loads from a downburst may be simulated. For a quasi-steady approach, the horizontal component is regarded as the dominant load in the outflow since the vertical velocity in the impingement region decreases to zero at the impingement plane.

3.3. Test facility

Boundary Layer Wind Tunnel 1 (BLWT1) at the University of Western Ontario is an open-circuit tunnel that is used to study wind loading on structures. The test section has a 33 m length, 2.4 m width, and a variable height (increases from ≈ 1.7 m at the inlet to ≈ 2.2 m at the outlet) to remove the streamwise pressure gradient. A computer-controlled turntable ($\phi 1.22$ m) allows yaw rotation of installed models for the study of flow incidence angle effects. A 30 kW motor draws ambient air through the working section by axial suction, generating a maximum test section velocity of 15 m/s. Honeycomb and screens at the tunnel inlet reduce turbulence intensity to $\approx 1\%$ in the test section freestream. BLWT1 is typically used for pressure, force balance, and aeroelastic testing of buildings, towers, bridges, and transmission lines.

Fig. 7 shows the basic components of the proposed downburst simulator installation. The slot jet originates from two centrifugal blowers mounted in the crawl space under the test section. Side inlets on each fan allow unobstructed inflow from both sides of the facility. The blower discharges are combined into a single flow with custom wide-angle diffusers that empty into ducting leading to the slot assembly. Due to space restrictions, the flow is turned through 180° to produce the slot jet through the nozzle (section 1 in Fig. 7). The depicted modifications are designed to be modular and removable, such that the facility is rapidly converted back to conventional boundary layer simulation mode.

The results in this article are from a preliminary proof-of-concept facility that is smaller than the proposed full-size BLWT1 outflow simulator by a factor of 6.75. Extensive details on the design and specifications of the prototype and full-size facilities are given in Lin (2005). Sizing of the drive unit and system components (e.g. screens) involves an iterative procedure similar to

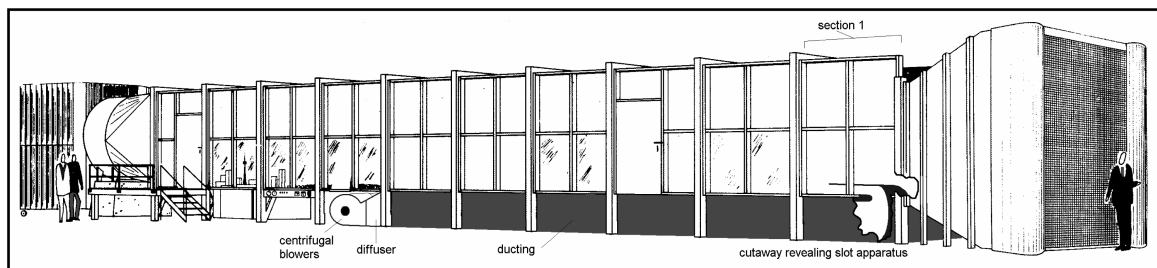


Fig. 7 Proposed modifications to UWO BLWT1 for downburst outflow simulation (adapted from original sketch by UWO BLWTL)

that used for pipe/duct flows. The design guidelines by Mehta (1977) for blower tunnels are incorporated.

3.4. Velocity profile measurements

Mean and turbulent velocity quantities are of primary interest, and crossed-hot-wire anemometry (HWA) is employed in this study. The Dantec MiniCTA 54T30 outputs are sampled with a National Instruments PCI-6071E data acquisition card (12-bit resolution). This measurement system has a frequency response up to 10 kHz. The following prototype facility results are from 30 s samples using a 1 kHz sampling rate.

A computer-controlled, two-axis traverse system allows fine positioning of the cross-wire probe. The traverse slides are controlled using stepper motors and the overall positioning accuracy of the probe wires in the following data is 0.2 mm. The measurement of a velocity profile is completely automated using LabVIEW.

Measurements of larger velocities are more certain with this system. Since slot jet velocity decays with distance from the slot exit, vertical profile maximum velocity (U_m) at smaller x/b have more certainty. The uncertainty on U_m is estimated as $\pm 7\%$ (± 1.7 m/s) at $x/b=50$ and $\pm 11\%$ (± 1.1 m/s) at $x/b=208$, for a 95% confidence level. Accuracy of the HWA and scale readability of the calibration manometry are considered. Relative accuracy, differential non-linearity, and gain error of the data acquisition card are also sources of systematic uncertainty. Repeatability, quantization, and noise are the random uncertainties considered.

4. Comparison of 2-D wall jet results to available 3-D data

Flow conditioning prior to the slot exit consisted of three wire mesh screens (total pressure loss coefficient of 4.6) located at the diffuser, fairings for the 180° bend from the anterior duct to the slot, and a contraction ratio of 9-to-1 for the duct and slot cross-sectional areas. As found in the high-precision facility of Gartshore and Hawaleshka (1964), the exit profile of the slot jet shows a larger boundary layer thickness on the bottom surface than the top surface of the slot. At the slot exit, the jet is nominally two-dimensional. Across the central 75% of the span, U variation is within $\pm 1.5\%$ of the spanwise mean. Slot exit streamwise turbulence intensity is less than 6%.

In the outflow simulator prototype, mean streamwise velocity profiles (variation of U in the z -direction) are measured at four distances downstream of the slot exit ($x/b=50, 100, 150,$ and 208). From the studies reviewed in Lin (2005), the plane slot jet should be developed at $x/b=50, 100,$ and $150,$ and is possibly losing its two-dimensionality at $x/b=208$. The exit velocity is 46 m/s and the slot jet Reynolds number is $Re_j=40100$. The working section ground plane is a smooth melamine surface.

The fluid mechanics convention is to normalize U by the vertical profile maximum (U_m), and z by the z -distance in the outer part of the wall jet at which $U=0.5 U_m$ (referred to as half-width, $z_{0.5}$), as illustrated in Fig. 6. However, in Fig. 8, z is normalized by z_m in order to compare the prototype facility measurements with full-scale data (Hjelmfelt 1988). It may also be argued that z_m is appropriate as a length scale for the region close to the ground, whereas $z_{0.5}$ is a better representation of eddies in the region above the downburst vertical profile maximum. The larger scatter for data at $x/b=150$ and 208 is likely due to higher uncertainty of the HWA for lower velocity measurements. U_m values are 25 m/s, 19 m/s, 14 m/s, and 10 m/s at the four x/b locations.

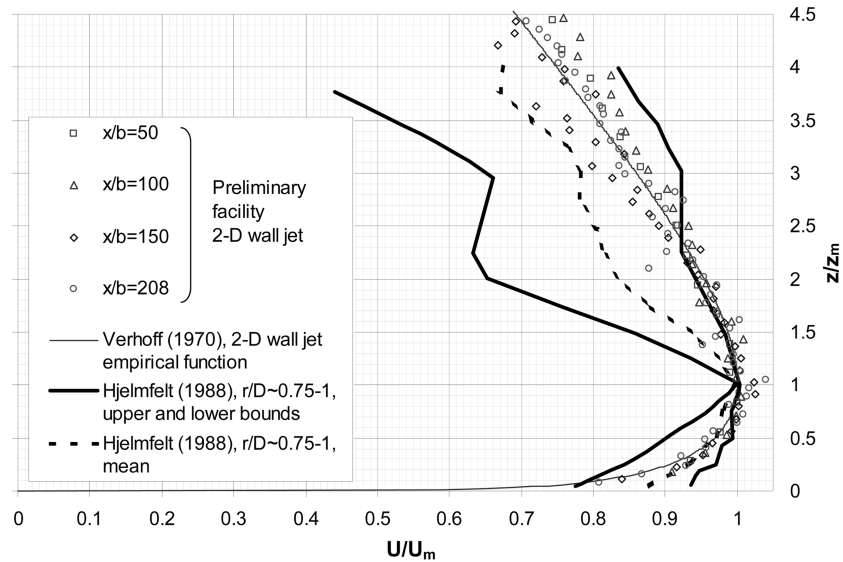


Fig. 8 Comparison of mean streamwise velocity profiles, for 2-D wall jets versus full-scale

Rather than simply taking U_m as the largest measured value without any consideration for experimental variability, the maximum value of a curve fit is taken as U_m . The form of the equation suggested by Verhoff (1970) for developed 2-D wall jets is used in the fitting procedure. Experimental scatter of some data points above the best-fit curve maximum results in some points exceeding $U/U_m = 1$ in Fig. 8. Nevertheless, the measured data shows general agreement with the empirical function suggested by Verhoff (1970). Verhoff found the constants in his empirical function from experiments where Re_j was less than a third of the present value, suggesting that the shape of downstream mean profiles is only weakly dependent on the slot jet Reynolds number. Verhoff’s function also matches the 2-D wall jet experimental results of other investigators, as reviewed by Lin (2005).

Hjelmfelt (1988) presents full-scale profiles of 8 downbursts from the JAWS field study. The upper and lower bounds on these profiles, and the mean, are shown in Fig. 8. As well, full-scale data from the NIMROD study is essentially identical to Hjelmfelt’s mean curve for points near the velocity maximum (Wood, *et al.* 2001). The 2-D wall jet profiles from the present study fall within the range of the full-scale profiles, and tend towards the upper bound.

Fig. 9 compares mean profiles for 2-D and 3-D wall jet experiments. Here, z is normalized by the half-width, as is commonly done for fundamental wall jet studies. Due to the jet growth, the half-width at $x/b = 208$ in the prototype facility is influenced by the upper boundary of the test section. Normalizing by a boundary-influenced half-width affects the profile at $x/b = 208$, so it is omitted from Fig. 9. Although normalizing by half-width is problematic at the largest x/b , it is done at the smaller x/b locations here in order to compare with previous results. In Fig. 8, z_m values at all x/b are far from and unaffected by the upper boundary of the test section.

The prototype facility data are represented fairly well by the developed 2-D wall jet empirical function (Verhoff 1970). Wood, *et al.* (2001) suggest a function of identical form for the mean radial velocity profile of the 3-D wall jet, based on their impinging jet results for $r/D_n \geq 1.5$. Both functions involve an exponent on $(z/z_{0.5})$ to account for the region beneath the profile maximum that

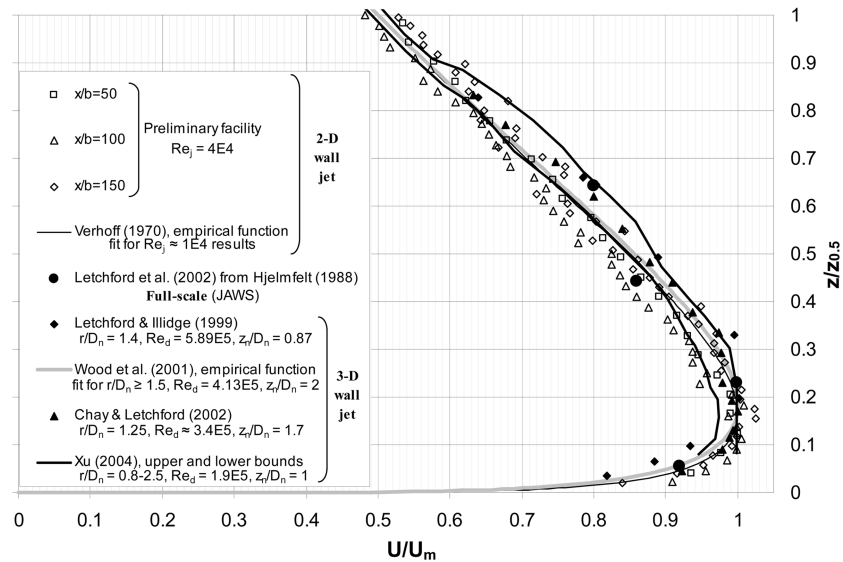


Fig. 9 Comparison of mean streamwise velocity profiles, for 2-D versus 3-D wall jets

resembles a boundary layer. Due to the exponent term ($1/7$ for 2-D versus $1/6$ for 3-D), the profile for the 2-D function is slightly more “full” near the wall than the 3-D one. Agreement is very good otherwise. Note that $r/D_n \approx 1$ is the radial distance at which previous investigators have reported maximum horizontal mean velocity, as indicated in Table 1.

Besides the agreement with Wood, *et al.* (2001), the representative 2-D wall jet profile (Verhoff 1970) also agrees well with developing region data from high- Re_d impinging jet experiments by Chay and Letchford (2002) and Xu (2004). Letchford and Illidge (1999) generate the downdraft using a wind tunnel with a non-circular cross-section, which may explain why their data are the poorest match to the 2-D data. In addition, radial confinement effects may be a concern because their flow was bounded on two sides by solid surfaces at $1.06 D_n$ and $1.29 D_n$. Xu (2004) found that a minimum radius of $8 D_n$ from the jet centreline is required to completely avoid perturbation of the surface pressure field by physical boundaries. The results from Letchford and Illidge (1999) are of interest though, because the outflow is one of the larger wall jets generated with an impinging jet.

The general agreement between the 2-D profiles and the full-scale results extracted from Hjelmfelt (1988) is encouraging, given that ground roughness effects have not been considered. All of the aforementioned results are from experiments that use a flat and smooth surface, which is the simplest terrain that a downburst outflow encounters. CFD and experiments indicate that profile shape is dependent on surface roughness (Wood, *et al.* 2001, Xu 2004, Choi 2004). Lin (2005) includes a preliminary investigation of roughness effects.

Given complete full-scale velocity time histories, it is still problematic to quantify the gustiness of a downburst outflow due to its strong transient nature. With a simple quasi-steady approach, it is recognized that the conventional definition of turbulence intensity does not properly account for the gustiness. However, in order to further compare the wall jet region of steady 3-D impinging jets and 2-D wall jets, the conventional statistical measures are used. Forthcoming work with the transient slot jet simulation will address this shortcoming.

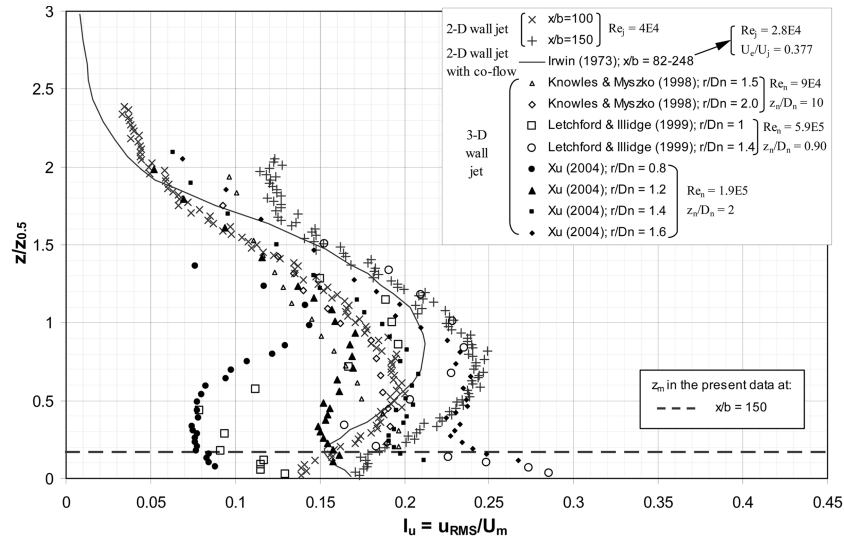


Fig. 10 Comparison of streamwise turbulence intensity profiles, for 2-D versus 3-D wall jets

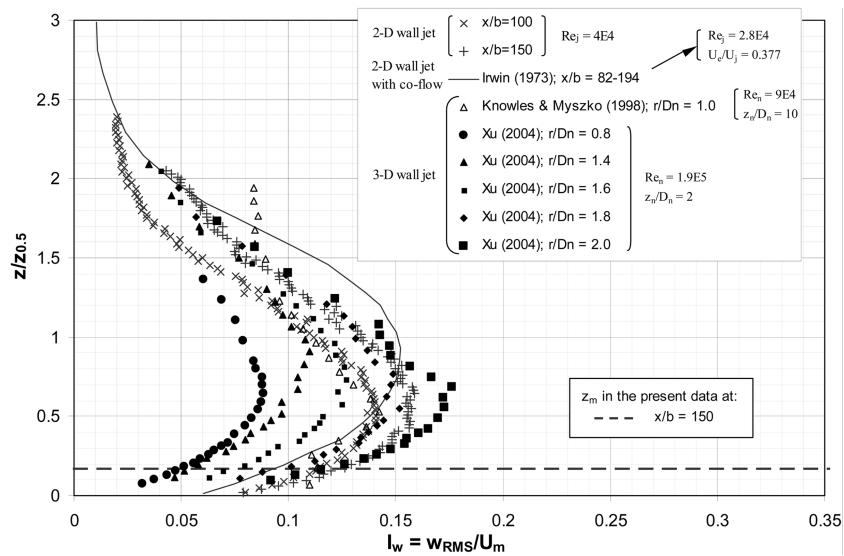


Fig. 11 Comparison of vertical turbulence intensity profiles, for 2-D versus 3-D wall jets

Figs. 10, 11 and 12 compare vertical profiles of the streamwise turbulence intensity, vertical turbulence intensity, and the dominant component of turbulent shear stress, respectively. The literature presents turbulence profiles using $z_{0.5}$ scaling (Irwin 1973, Knowles and Myszko 1998, Letchford and Illidge 1999, Xu 2004), so this convention is retained here. Note that values of $z_m/z_{0.5}$ are known (Launder and Rodi 1981) and may be used for conversion to z_m scaling, but such re-scaling does not add any new information.

It may be seen that although the 2-D slot jet mean profiles reach a fully developed state at $x/b=100$ and 150, the turbulence profiles do not. There is no clear consensus amongst previous workers

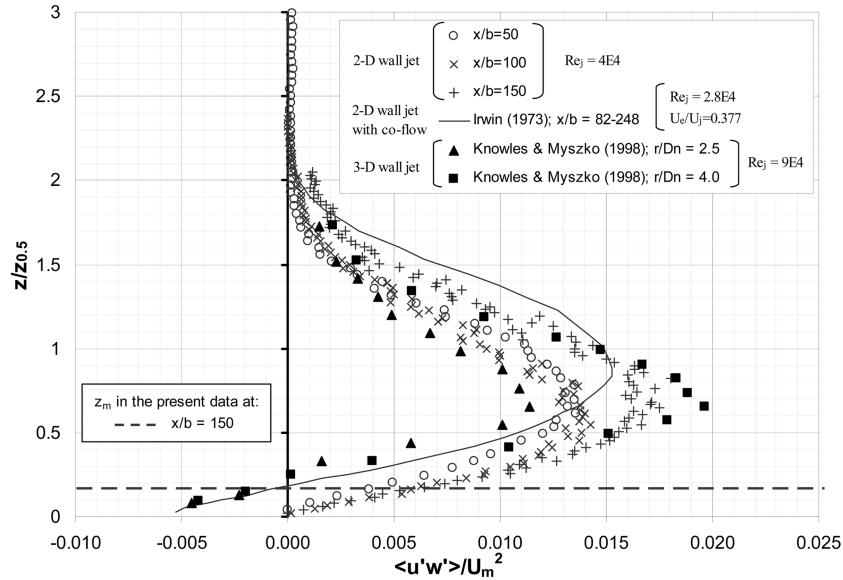


Fig. 12 Comparison of turbulent shear stress profiles, for 2-D versus 3-D wall jets

regarding similarity of the turbulence profiles. Wygnanski, *et al.* (1992) do not find similarity for $x/b=60-120$ and $Re_j=5000-19000$. Abrahamsson, *et al.* (1994) find similarity for $x/b=70-150$ and $Re_j=10000-20000$, but their tunnel was completely blocked off above the slot nozzle (i.e., where the co-flow enters the working section in Fig. 6 at $x/b=0$). The mean velocity profiles in these two studies match well.

Fig. 10 indicates that I_u profiles in the fully-developed region of the 2-D wall jet are comparable to the 3-D wall jet profiles at $r/D_n=1.4$ and 1.6 (Xu 2004), and at $r/D_n=2.0$ (Knowles and Myszko 1998). Although the most intense winds in full-scale occur at slightly smaller radial distance, I_u in the self-similar region of the 2-D wall jet shows quite good agreement with I_u in the developing region of the 3-D wall jet. Notably, the 3-D wall jet profiles show an increase in I_u close to $z=0$, which is not seen in the present 2-D wall jet data. The 2-D wall jet with co-flow from Irwin (1973) does show this increase close to the wall though. The horizontal dashed line gives an indication of the height of interest - the location of the maximum in the vertical profile of mean streamwise velocity in the developed 2-D wall jet.

Below $z/z_{0.5}=1$, the profiles by Letchford and Illidge (1999) each vary over a larger range of I_u than the other results. The impinging jet laboratory data from Poreh, *et al.* (1967) has been used in the literature for comparison to downbursts. However, they measured turbulence quantities in the developed region only ($r/D_n > 9$) and used a very large nozzle height ($z/D_n = 12$).

Figs. 11 and 12 show good agreement in profile shape between the 2-D and 3-D wall jet for vertical turbulence intensity and turbulent shear stress, respectively. Near where the maximum in the mean profile occurs, the I_w profiles for the developed 2-D wall jet match the I_w profiles for the developing 3-D wall jet ($r/D_n=1.0$ for Knowles and Myszko 1998 and $r/D_n=2.0$ for Xu 2004). Turbulent shear stress profiles in the fully-developed region of the 2-D wall jet match the 3-D wall jet profiles at larger radial distance than for the I_u and I_w profiles - but the matching profiles are still in the region where the turbulence quantities of the 3-D wall jet are still developing ($r/D_n < 4.5$,

Table 2 Estimated scaling of present approach and other studies

Experiment	Geometric scale	Velocity scale	Comments
3-D impinging jet			
Letchford and Illidge (1999)	1:400 - 1:2000	1:3.3 - 1:7.5	Steady jet from wind tunnel exit (octagonal cross-section).
Wood, <i>et al.</i> (2001)	1:1300 - 1:6500	1:1.6 - 1:3.8	Steady jet from circular nozzle.
Chay and Letchford (2002)	1:800 - 1:3900	1:3.3 - 1:7.5	Steady jet from circular nozzle with 5 cm lip.
Xu (2004)	1:1800 - 1:9300	1:2.5 - 1:5.8	Steady jet from large circular pipe.
2-D slot jet			
Prototype facility	1:280 - 1:1400	1:3.3 - 1:7.7	Based on current HWA results.
Full-size facility (BLWT1)	1:60 - 1:300	1:3.3 - 1:7.5	Based on predicted values for z_m and U_m at $x/b=208$.

Knowles and Mysko 1998).

It is apparent that the radial location where the maximum level of turbulence intensity occurs does not coincide with the radial location where the maximum mean velocity occurs. As the mean velocity decays with distance from the jet origin, fluctuations are expected to be more significant relative to the local mean velocity. In terms of simulating a translating event with the present approach, it is encouraging that the profiles for the 2-D wall jet with co-flow have comparable magnitude and shape as the other cases, for streamwise and vertical turbulence intensity as well as turbulent shear stress.

5. Estimated model scale

Table 2 shows the estimated model scale of the flow in the prototype and full-size slot jet facilities for downburst outflow simulation. The model scale of impinging jet simulations is estimated by relating the nozzle diameter to full-scale downdraft diameter. Although a nominal value is occasionally stated, a range of scales is more appropriate since downdraft diameter is variable from event to event.

The field data in Table 1 suggests that strong downbursts have a downdraft diameter of less than 2000 m. As well, Fujita (1981) defined the smallest downbursts as having a diameter of at least 400 m. These two values and the nozzle diameter yield the geometric scale ranges, given in Table 2, for the impinging jet simulations.

Neglecting the downdraft region requires the model scale to be estimated based on the flow, rather than the physical geometry of the apparatus. Based on $z_m/D \approx 2.5\%$ at the radial location in the Yorkville downburst where the maximum outflow velocity is expected (see Table 1), z_m at a desired test location in the facility may be related to a corresponding downdraft diameter. For example, $z_m = 0.035$ m at $x/b = 208$ in the prototype facility. This height-to-maximum-velocity corresponds to a 1.4 m downdraft diameter. Relating this value to downdraft diameters of 400 m and 2000 m, the prototype facility outflow is estimated as being 280-1400 times smaller than actual downburst outflows.

The outflow from the full-size facility is expected to be an order of magnitude larger than in

previous simulations. At the turntable location in the BLWT1 outflow simulator, z_m will be ≈ 0.17 m. This is a reasonable size at which to construct complex building or lattice tower models.

The velocity scale range in Table 2 is based upon 32.5 and 75 m/s - the former being the lowest wind speed where moderate structural damage is expected (Fujita 1981) and the latter being an estimate of the largest attainable velocity by a downburst⁴ (Fujita 1985). Positioning the test model closer to the slot jet will result in larger wind loads. However, this comes at the cost of a smaller z_m .

6. Validity of the 2-D assumption for an idealized outflow

To evaluate the accuracy of approximating a 3-D downburst outflow with a 2-D wall jet, the geometry in Fig. 13 is examined. The idealized outflow from a stationary downburst spreads radially outwards from a central stagnation point. To investigate the importance of downburst front curvature on the resultant wind loading of a structure, one-half times the transverse width of the structure is denoted as m and the distance of the exposed face from the downburst stagnation point is denoted as r .

From the perspective of the exposed face, the largest distance that a 3-D outflow lags behind a corresponding 2-D downburst front, is the lag distance (r^*) at the transverse ends of the exposed face. In other words, a small r^* for a specified transverse width implies that frontal curvature has little effect on the wind load that the exposed face experiences. The lag distance is a function of structure width and location, as shown by Eq. (1).

$$r^* = \sqrt{m^2 + r^2} - r \quad (1)$$

The lag distances, for various combinations of structure location and exposed width, are shown in Table 3 as a percentage of r . The lag distance is insignificant for exposed widths of typical structures. Savory, *et al.* (2001) considered 9.1 m as the width of a free-standing lattice tower of 50.5 m height; other common tower designs are smaller. The range of exposed widths (2-m) in Table 3 covers multiple conductor spans of a transmission line system. If a lag distance of less than 2% of the shortest distance from the exposed face to the stagnation point is an acceptable downburst front curvature effect, the lower left unshaded values in Table 3 indicate that the 2-D

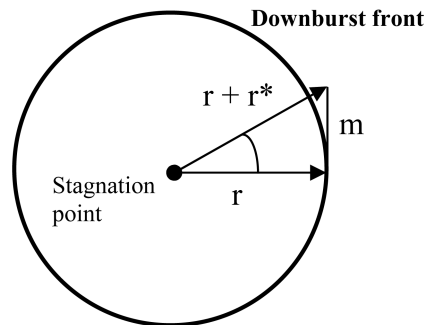


Fig. 13 Plan view of a downburst outflow

⁴Fujita projected JAWS and NIMROD data to estimate annual downburst frequency for the contiguous U.S.A. The estimated annual frequency becomes less than one at approximately 75 m/s, as shown in Fig. 2.

Table 3 Lag distance as a percentage of the distance of the exposed structure from the stagnation point

r [m]	$2 \cdot m$ [m]							
	10	100	200	300	400	500	1000	2000
250	0.020	2.0	7.7	17	28	41	124	312
500	0.005	0.5	2.0	4.4	7.7	12	41	124
750	0.002	0.2	0.9	2.0	3.5	5.4	20	67
1000	0.001	0.1	0.5	1.1	2.0	3.1	12	41
1250	0.001	0.08	0.3	0.7	1.3	2.0	7.7	28
1500	0.0006	0.06	0.2	0.5	0.9	1.4	5.4	20
1750	0.0004	0.04	0.2	0.4	0.7	1.0	4.0	15
2000	0.0003	0.03	0.1	0.3	0.5	0.8	3.1	12

assumption is valid for wide structures located far from the stagnation point. For an event with $D=1000$ m, the high-intensity region is near $r=1250$ m. For a 500 m transmission line section subjected to this outflow, curvature effects are not expected to be very significant and a 2-D approach appears reasonable.

One may expect frontal curvature to be less important and the 2-D assumption to be more valid in the outflow of a translating downburst than in a stationary one, due to the pronounced directionality of the former. If so, the next progression is to approximate the outflow as emitting from a line source rather than a central point source. In that case, the validity of the 2-D assumption may be examined by considering the divergence of velocity.

Expressing the horizontal divergence of velocity in the coordinate system and variables shown in Fig. 14, Eq. (2) is reworked as the sum of longitudinal and transversal components shown as Eq. (3):

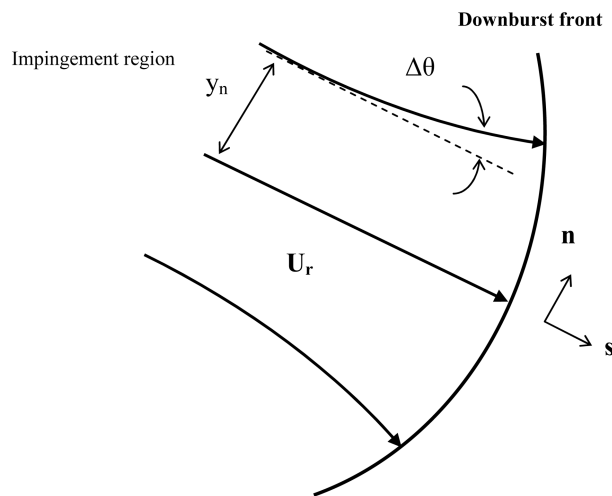


Fig. 14 Plan view of the downburst outflow in a normal-radial coordinate system

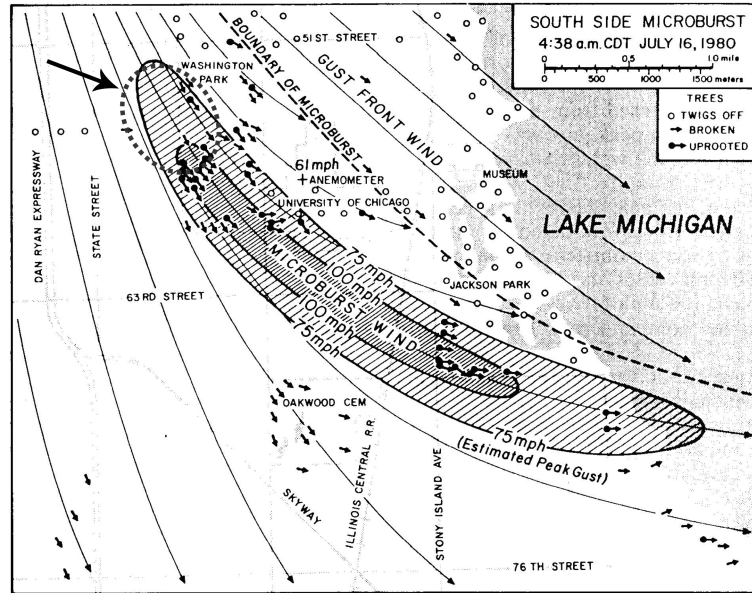


Fig. 15 Damage swath of a translating downburst (reproduced from Fujita and Wakimoto 1981 with dashed circle added)

$$\nabla_h \cdot \vec{U} = \frac{\partial u}{\partial x} + \frac{\partial v}{\partial y} \quad (2)$$

$$\nabla_h \cdot \vec{U} = \frac{\partial U_r}{\partial s} + U_r \frac{\partial \theta}{\partial n} \quad (3)$$

= longitudinal divergence + transversal divergence (diffuence)

Following the treatment of the thunderstorm gust front by Wakimoto (1982), the values listed below are used to estimate $\Delta\theta$ at which the diffuence term becomes significant with respect to the longitudinal divergence term. The following values are estimated from the region within the dashed circle in Fig. 15.

- $\Delta U_r = 11.2 \text{ m/s}$ (25 mph)
- $\Delta s = 900 \text{ m}$ (approximate longitudinal extent of circled region)
- $y_n = 400 \text{ m}$ (approximate transverse extent of the hatched region)
- $U_r = 39.1 \text{ m/s}$ (average of 75 and 100 mph)

The resulting longitudinal divergence is on the order of 0.01 s^{-1} .

Table 4 indicates that the diffuence is one order of magnitude smaller than the longitudinal divergence only for small angular deviations of the flow from the s -direction. This first-order analysis is highly dependent on the estimated parameters from the available field data. Wakimoto (1982) shows the 2-D assumption is a good approximation for gust fronts, which are generally at least an order of magnitude larger than downburst outflows (Charba 1974). Diffuence is more than an order of magnitude smaller than longitudinal divergence for $\Delta\theta = 15^\circ$, for a gust front with $y_n = 20 \text{ km}$.

Table 4 Significance of diffluence for an outflow from a translating downburst (0.8 km wide front)

$\Delta\theta$ [°]	Diffluence [s^{-1}]	Transverse/longitudinal divergence ratio
1	0.002	0.1
2	0.003	0.3
3	0.005	0.4
4	0.007	0.5
5	0.009	0.7

Table 5 Significance of diffluence for an outflow from a downburst line (17 km length)

$\Delta\theta$ [°]	Diffluence [s^{-1}]	Transversal/longitudinal divergence ratio
10	0.0003	0.03
20	0.0006	0.07
30	0.0008	0.10
40	0.0011	0.14
50	0.0014	0.17

The JAWS field campaign identified simultaneous occurrence of multiple downbursts in line formation, which are referred to as “microburst lines” by Hjelmfelt (1988)⁵. Continuous occurrence of the individual downbursts at their respective locations allowed downburst lines to persist for over two hours. Hjelmfelt (1988) reported an average line length of 17 km based on 20 cases. Depending on the proximity of the individual downbursts to each other, the outflow is described as being homogeneous or discrete. Half of the lines studied were homogeneous and half were discrete. The exact outflow velocity profile depends on the spacing and strengths of the individual downbursts.

Clearly, the 2-D assumption is more valid for a downburst line than an isolated event. The comparison of diffluence to longitudinal divergence is done for a downburst line using the parameters reported by Hjelmfelt (1988). Table 5 suggests that the effect of diffluence in a downburst line is weak even with large angular deviations of the flow from the s -direction.

7. Conclusions

As seen from recent review of convective downdrafts (Wakimoto 2001), meteorologists are making efforts toward a complete understanding of thunderstorms and how Fujita’s concept of a downburst fits into the parent convective system. The difficulty of investigating intense downburst outflows in the field has led to laboratory simulations as an additional means to gain insight. Previous downburst simulations have helped clarify the structure and morphology of the phenomenon. The impinging jet and released fluid models have served well in this regard. However, scaling considerations dictate that it is not very practical to generate a large-scale outflow using these approaches. The present work addresses the problem of generating a flow that is like a downburst outflow and is of sufficient size to allow aeroelastic testing of structure models. The

⁵Downburst clusters produced by extratropical mesoscale convective weather systems are also referred to as “derechos” (Wakimoto 2001)

proposed slot jet approach has the advantage of being readily extended to transient simulations and to include more complex configurations beyond a stationary downburst.

Present results show that time-averaged outflow wind speed profiles can be reproduced quite well with a slot jet approach. Direct matching of the developed 2-D wall jet profiles with profiles in the intense flow region of 3-D wall jets shows good agreement. The turbulence quantity profiles of the developed 2-D wall jet match the corresponding profiles from the developing 3-D wall jet slightly downstream of where maximum radial mean velocity is observed in the field. In other words, the turbulence quantities of the 2-D jet are slightly higher than desired. In the full-size facility, flow conditioning may help to refine the profiles, which will be several times larger in size than previous approaches have generated.

In terms of frontal curvature effects, the present analysis finds that it is valid to approximate a 3-D outflow with a 2-D assumption for multiple spans of a transmission line. The present findings agree with those of Mason, *et al.* (2005), who suggest that the downburst front is reasonably flat with transverse distance. The exposed width of the structure and its location relative to the downburst impingement point are key parameters for wind loading based on the axisymmetric, isolated downburst model.

The rear-flank downdraft (RFD) appears to be “the strongest downdraft associated with the supercell” (Wakimoto 2001). RFDs may be more like a small gust front, as opposed to the axisymmetric column of descending air envisioned by Fujita. The axisymmetric model seems to match descriptions of forward-flank downdrafts, rather than RFDs. Data from the 4 June 2002 RFD near Lubbock, Texas (Gast and Schroeder 2003) indicate that frontal curvature is negligible over a span of 1578 m, at 3 m to 15 m height AGL. Wind speed time histories are well-correlated across the span. The irrelevance of frontal curvature for the strongest impinging convective downdrafts would support the validity of a 2-D modelling approach.

It may be pointed out that a quasi-steady model does not account for some of the features of the downburst outflow. It inherently loses some exact details of the flow, as it is intended to be a simplified model to aid practitioners and designers. The relevant question is whether or not all of these details need to be considered in design of structures. Is dynamic response significant in downburst wind loading of particular structures? Is it sufficient to simply simulate the mean profile in a quasi-steady manner to capture the essential differences between wind loading from a downburst outflow and the conventional ABL? Introducing a slot jet into the working section of a conventional boundary layer wind tunnel and its extension to a transient simulation will provide insight into these questions.

Acknowledgements

Manitoba Hydro, Natural Sciences and Engineering Research Council of Canada, and the Institute for Catastrophic Loss Reduction provided financial support for this work. The UWO University Machine Shop fabricated parts for the experimental facility. Some test equipment was kindly made available by Dr. G. A. Kopp and Dr. R. J. Martinuzzi. C. Novacco aided with data acquisition and post-processing of HWA data. Dr. J. D. Holmes provided helpful feedback and insight.

References

Abrahamsson, H., Johansson, B., and Löfdahl, L. (1994), “A turbulent plane two-dimensional wall-jet in a

- quiescent surrounding”, *Euro. J. Mech., B/Fluids*, **13**(5), 533-556.
- Alahyari, A. and Longmire, E. K. (1995), “Dynamics of experimentally simulated microbursts”, *AIAA J.*, **33**(11), 2128-2136.
- American Society of Civil Engineers (1999), “Wind tunnel studies of buildings and structures”, ASCE Manuals and Reports on Engineering Practice No. 67, second edition, editor: N. Isyumov, publisher: ASCE.
- Charba, J. (1974), “Application of gravity current model to analysis of squall-line gust front”, *Mon. Weather Rev.*, **102**, February, 140-156.
- Chay, M. T. and Letchford, C. W. (2002), “Pressure distributions on a cube in a simulated thunderstorm downburst-Part A: Stationary downburst observations”, *J. Wind Eng. Ind. Aerodyn.*, **90**, 711-732.
- Choi, E. C. C. (2004), “Field measurement and experimental study of wind speed profile during thunderstorms”, *J. Wind Eng. Ind. Aerodyn.*, **92**, 275-290.
- Choi, E. C. C. and Hidayat F. A. (2002), “Dynamic response of structures to thunderstorm winds”, *Prog. Struct. Eng. Mater.*, **4**, 408-416.
- Cook, N. J. (1973), “On simulating the lower third of the urban adiabatic boundary layer in a wind tunnel”, *Atmos. Env.*, **7**, 691-705.
- Förthmann, E. (1934), “Über turbulente Strahlausbreitung”, *Ing. Arch. (Arch Appl. Mech.)*, **5**(1), 42-54. Translated as: “Turbulent jet expansion”, NACA Technical Memorandum #789, March 1936.
- Fujita, T. T. (1981), “Tornadoes and downbursts in the context of generalized planetary scales”, *J. Atmos. Sci.*, **38**(8), 1511-1534.
- Fujita, T. T. (1985), “The downburst: Microburst and macroburst”, University of Chicago, Department of Geophysical Sciences, Satellite and Mesometeorology Research Project, Research Paper #210.
- Fujita, T. T. (1990), “Downbursts: Meteorological features and wind field characteristics”, *J. Wind Eng. Ind. Aerodyn.*, **36**, 75-86.
- Fujita, T. T. and Wakimoto, R. M. (1981), “Five scales of airflow associated with a series of downbursts on 16 July 1980”, *Mon. Weather Rev.*, **109**, 1439-1456 July.
- Gartshore, I. and Hawaleshka, O. (1964), “The design of a two-dimensional blowing slot and its application to a turbulent wall jet in still air”, McGill University, McGill Engineering Research Laboratory, Technical Note 64-5 June.
- Gast, K. D. and Schroeder, J. L. (2003), “Supercell rear-flank downdraft as sampled in the 2002 thunderstorm outflow experiment”, *Proceedings of the 11th International Conference on Wind Engineering*, Lubbock, TX, USA, 2-5 June, 2233-2240.
- Hjelmfelt, M. R. (1988), “Structure and life cycle of microburst outflows observed in Colorado”, *J. Appl. Meteorol.*, **27**, 900-927.
- Hjelmfelt, M. R. (2003), “Microbursts and their numerical simulation”, *Preprints of the Harold D. Orville Symposium*, Rapid City, SD, USA, 26 April, 51-67. Available from: Institute of Atmospheric Sciences, South Dakota School of Mines and Technology, USA.
- Holmes, J. D. (1992), “Physical modelling of thunderstorm downdrafts by wind-tunnel jet”, *Australian Wind Engineering Society Second Workshop on Wind Engineering*, Melbourne, Australia, 20-21 February.
- Holmes, J. D. (1999), “Modelling of extreme thunderstorm winds for wind loading of structures and risk assessment”, *Wind Engineering into the 21st Century, Proceedings of the 10th International Conference on Wind Engineering*, Copenhagen, Denmark, 21-25 June, publisher: Balkema, Netherlands, 1409-1415.
- Holmes, J. D. (2001), *Wind Loading of Structures*, Spon Press, New York, NY, USA.
- Holmes, J. D. and Oliver, S. E. (2000), “An empirical model of a downburst”, *Eng. Struct.*, **22**, 1167-1172.
- Irwin, H. P. A. H. (1973), “Measurements in a self-preserving plane wall jet in a positive pressure gradient”, *J. Fluid Mech.*, **61**(1), 33-63.
- Knowles, K. and Myszkowski, M. (1998), “Turbulence measurements in radial wall-jets”, *Exp. Therm. Fluid Sci.*, **17**, 71-78.
- Lauder, B. E. and Rodi, W. (1981), “The turbulent wall jet”, *Prog. Aerospace Sci.*, **19**, 81-128.
- Letchford, C. W. and Illidge, G. (1999), “Turbulence and topographic effects in simulated thunderstorm downdrafts by wind tunnel jet”, *Wind Engineering into the 21st Century, Proceedings of the 10th International Conference on Wind Engineering*, Copenhagen, Denmark, 21-25 June, publisher: Balkema, Netherlands, 1907-1912.

- Letchford, C. W., Mans, C., and Chay, M. T. (2002), "Thunderstorms - their importance in wind engineering (a case for the next generation wind tunnel)", *J. Wind Eng. Ind. Aerodyn.*, **90**(12-15), 1415-1433.
- Lin, W. E. (2005), "Large-scale physical simulation of a microburst outflow using a slot jet", University of Western Ontario, MEng thesis, December.
- Lundgren, T. S., Yao, J., and Mansour, N. N. (1992), "Microburst modelling and scaling", *J. Fluid Mech.*, **239**, 461-488.
- Mara, T. G. and Galsworthy, J. K. (2006), Private Communications.
- Mason, M., Letchford, C. W., and James, D. (2003), "Pulsed jet simulation of a thunderstorm downburst", *Proceedings of the 11th International Conference on Wind Engineering*, Lubbock, TX, USA, 2-5 June, 2249-2256.
- Mason, M. S., Letchford, C. W., and James, D. L. (2005), "Pulsed wall jet simulation of a stationary thunderstorm downburst, Part A: Physical structure and flow field characterization", *J. Wind Eng. Ind. Aerodyn.*, **93**, 557-580.
- Mehta, R. D. (1977), "The aerodynamic design of blower tunnels with wide-angle diffusers", *Prog. Aero. Sci.*, **18**, 59-120.
- Nicholls, M., Pielke, R., and Meroney, R. (1993), "Large eddy simulation of microburst winds flowing around a building", *J. Wind Eng. Ind. Aerodyn.*, **46 & 47**, 229-237.
- Poreh, M., Tsuei, Y. G., and Cermak, J. E. (1967), "Investigation of a turbulent radial wall jet", *J. Appl. Mech.*, **34**, 457-463.
- Proctor, F. H. (1988), "Numerical simulations of an isolated microburst. Part I: Dynamics and structure. *J. Atmos. Sci.*, **45**(21), 3137-3160.
- Sarkar, P. P. and Haan, Jr., F. L. (2002), "Next generation wind tunnels for simulation of straight-line, thunderstorm- and tornado-like winds", *Proceedings of the 34th Joint Meeting of the U.S.-Japan Panel on Wind and Seismic Effects*, Gaithersburg, MD, USA, 13-15 May.
- Savory, E., Parke, G. A. R., Zeinoddini, M., Toy, N., and Disney, P. (2001), "Modelling of tornado and microburst-induced wind loading and failure of a lattice transmission tower", *Eng. Struct.*, **23**, 365-375.
- Selvam, R. P. and Holmes J. D. (1992), "Numerical simulation of thunderstorm downdrafts", *J. Wind Eng. Ind. Aerodyn.*, **41-44**, 2817-2825.
- Verhoff, A. (1970), "Steady and pulsating two-dimensional turbulent wall jets in a uniform stream", Princeton University, PhD thesis.
- Wakimoto, R. M. (1982), "The life cycle of thunderstorm gust fronts as viewed with Doppler radar and rawinsonde data", *Mon. Weather Rev.*, **110**, 1060-1082.
- Wakimoto, R. M. (2001), "Convectively driven high wind events", *Severe Convective Storms, Meteor. Monogr.*, **50**, 255-298. American Meteorological Society. Editor: C.A. Doswell III.
- Wilson, J. W., Roberts, R. D., Kessinger, C., and McCarthy, J. (1984), "Microburst wind structure and evaluation of Doppler radar for airport wind shear detection", *J. Climate Appl. Meteorol.*, **23**, 898-915.
- Wilson, J. W. and Wakimoto, R. M. (2001), "The discovery of the downburst: T. T. Fujita's contribution", *Bull. Amer. Meteorol. Soc.*, **82**(1), January, 49-62.
- Wood, G. S., Kwok, K. C. S., Motteram, N. A., and Fletcher, D. F. (2001), "Physical and numerical modelling of thunderstorm downbursts", *J. Wind Eng. Ind. Aerodyn.*, **89**, 535-552.
- Wynanski, I., Katz, Y., and Horev, E. (1992), "On the applicability of various scaling laws to the turbulent wall jet", *J. Fluid Mech.*, **234**, 669-690.
- Xu, Z. (2004), "Experimental and analytical modeling of high intensity winds", University of Western Ontario, PhD thesis, December.
- Yao, J. and Lundgren, T. S. (1996), "Experimental investigation of microbursts", *Exp. Fluids*, **21**, 17-25.